Some Useful Application of Expanded Graphite : Review

Young-Shin Ko[1], Won-Chun Oh[2, 1†]

[1]*Young Company Co., Seosan-si, Chungnam-do, Korea, 356-706*
[2]*Department of Advanced Materials Science & Engineering, Hanseo University, Seosan-si, Chungnam-do, Korea, 356-706*

Abstract: The modified expanded graphite (MEG) powder was used as some kinds of materials in terms of application. Expanded graphite (EG) prepared from natural graphite by chemical treatment, kept most excellent characteristics of natural graphite and overcame hard, fragile and some other defects of natural graphite. EG was usually used to improve the conductivities of some high polymer materials. The electrical conductive networks, in which electrons could move freely, finally formed when the distant among conductive particles have been shorten because of the increment of EG content and the electrical properties of composites, meanwhile, could be adjusted by changing EG content in a wide percentage range. We described that the expanded graphite is also an excellent material for antistatic and antielectromagnetic with some useful analytical data.

1. General

Graphite is the most stable allotrope carbon, due to the carbon bonding involves sp^2 (trigonal) hybridization. It consists of carbon layers (known as graphere layers) with covalent bonding within each layer. And, they are linked by a weak van der Walls interaction produced by a delocalized π-orbital [1]. The special sandwich structure and long distance between the carbon layers make it easy to insert atoms or molecules between the carbon layers. For the obtaining of porous expanded graphite (EG), they need heating of the graphite intercalation compounds (GICs), which induces the vaporization of the intercalated species and hence, a significant expansion of the material along the crystallographic c-axis occurs. The morphology and pore structure of EG can be determined by altering preparation conditions, and there are many reports on preparation procedures, pore structure and application of EG [2–4]. EG is a highly porous worm-like and very light material with typical apparent densities of 0.002–0.01 gcm^{-3}, and is a material of growing importance because of numerous actual and potential applications in hydrogen storage [5], fuel cell [6], sensor [7], catalyst [8], biomedical materials [9] and adsorbent. The absorbing spaces of EG can be divided into two types. One is the wrapping absorption space (WAS) constructed by EG stacking on each other; the second is the pores in each EG worm-like segment [10].

† Corresponding author: *wc_oh@hanseo.ac.kr*

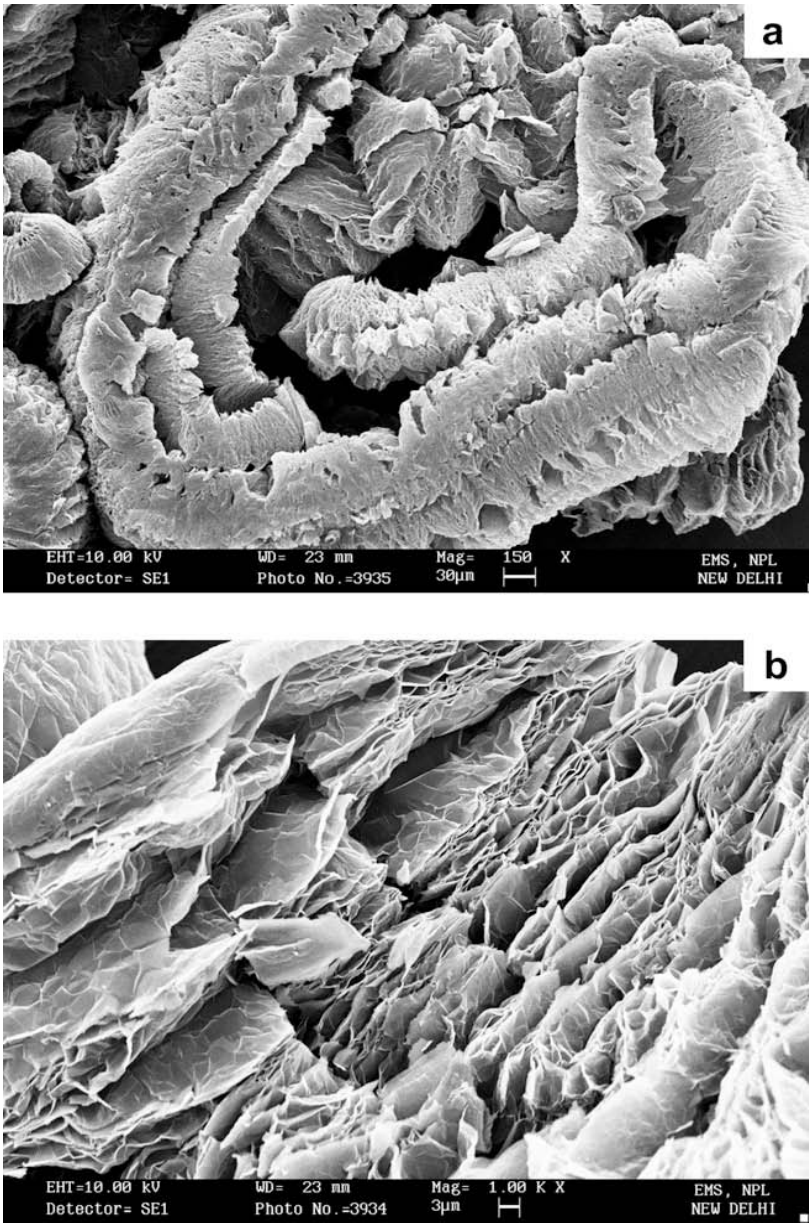

Figure 1: SEM micrograph of expanded graphite [11].

Fig. 1a shows the SEM micrograph of EG. This is vermiform in shape with loose and porous structure that is due toopening of planar carbon networks wedged at the edge surface of crystallite by surface groups as a consequence of oxidation. The higher magnification (Fig. 1b) is clearly seen the graphite flakes interlayer spacing, due to separation of increased distance and leads into porous structure. In the expansion process, destruction

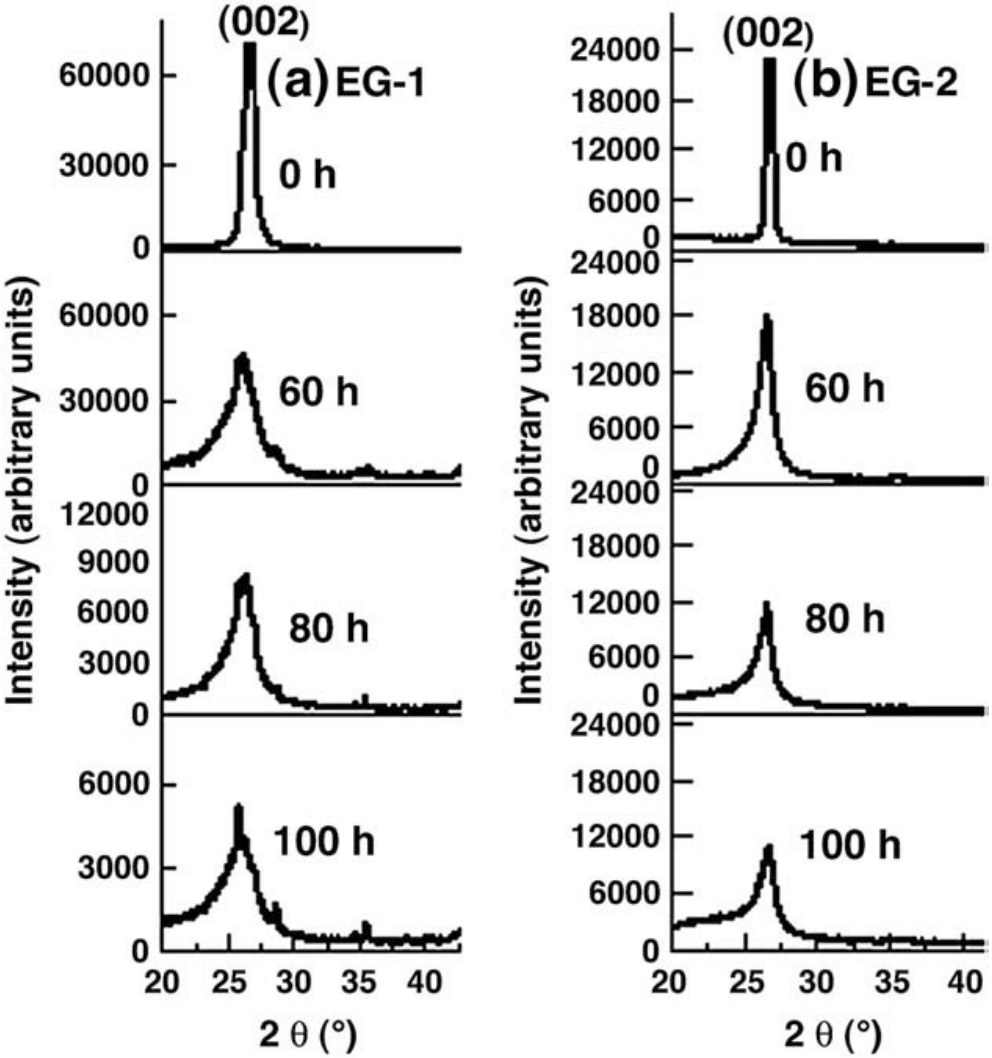

Figure 3: XRD patterns of (002) diffraction peaks of (a) EG-1 and (b) EG-2 as a function of milling time.[13]

of graphite crystal structure causes consequence expansion in the c-direction. This scale is about hundred times and resulted in an enormous increase in volume as a consequence of sudden evaporation of intercalate. After expansion, EG emerges as a loose structure and porous material consisting of numerous graphite sheets of thickness in nanometers and micrometer in diameter. This structure is affect to EG physical properties with high surface area, corresponding to graphite nanosheets having thickness between 50–100 nm.

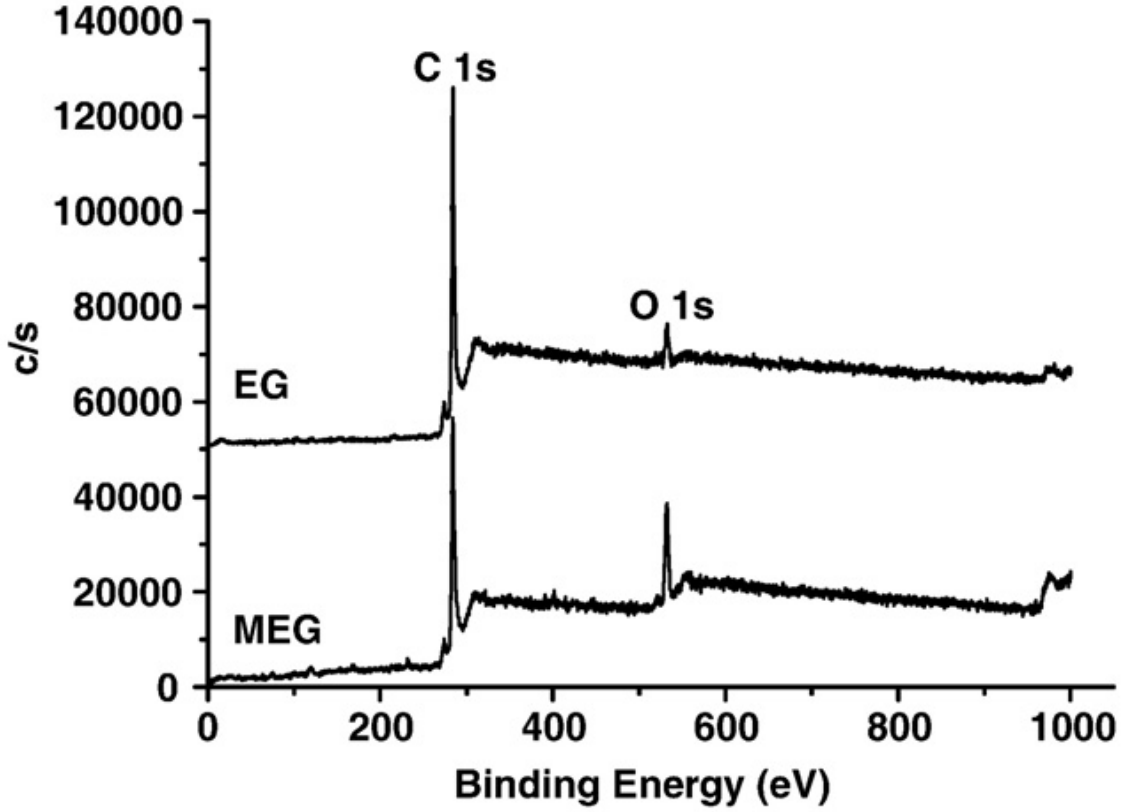

Figure 2: XPS survey spectra [12].

It is clear that the surface oxygen element content increased and the surface carbon element content decreased after the second oxidation from the X-ray photoelectron spectroscopy (XPS) analysis (Fig. 2). It also indicated that the polar groups containing oxygen element were introduced in the second oxidation [12].

2. Application

2.1 Milling properties : Microstructure Evolution Characterized by XRD

Fig. 3 shows the XRD patterns of (002) diffraction peaks of EG-1 (a) and EG-2 (b) after various milling times. The (002) diffraction peaks are broadened asymmetrically with increasing the milling time, similar to that found in ball-milled natural graphite [14,15]. This may relate to a reduction in the crystallite thickness in c-direction (Lc), or introduction of disordered graphene planes during the milling process [15]. For EG-1, two non-graphite peaks at 28.6 and 35.6° appear after 60 h milling and become stronger with prolonging the milling time,

as shown in Fig. 3a. This seems to be a crystalline phase evolution of EG-1, but which is not the case for EG-2. The Lc is calculated by comparing the profile width of a standard profile (silicon power) with a sample profile. Therefore, the structural broadening is calculated by $\beta=\beta_{observed}-\beta_{standard}$ [16]. It is well known that EG can be compressed into flexible graphite sheets having superior flexibility and compressibility [17]. Therefore, we assume that huge amounts of thin flexible graphite sheets are produced during the milling process due to the impact of milling balls on EG. According to Ref. [18], the expansion volume of EG increases with increasing the expansion temperature of expandable graphite from 600 to 1000 °C (here EG-1 and EG-2 exhibit expansion volumes of 70 and 250 ml/g, respectively), and the growth of pores inside the worm-like particles of EG at 1000 °C is far more complete compared with that at 600 °C. We believe that the flexibility of the thin flexible graphite sheets caused by ball milling is associated with the expansion volume and the growth of pores inside the EG particles, and the flexibility of the thin flexible graphite sheets of EG-2 are higher than that of EG-1. Therefore, EG-2 exhibits lower Lc evolution degree than EG-1 does during the milling process.

2.2 Polymer blending – mechanical properties

The stressestrain and impact tests were carried out on selected samples at room temperature after previous conditioning (see experimental). Fig. 4a and b shows the mechanical properties of neat PLA compared to composites in which the amount of nanofiller (EG) is up to 12%. On one hand, both stress (given as maximum tensile strength) and nominal strain at break of neat PLA are gradually decreasing in composites by increasing the percentage of EG. However, the lower tensile strength can be attributed to the inevitable aggregation and to the quality of dispersion that becomes poorer at higher percentage of nanofiller. When added with 4% EG, the resulting PLA-based compositions could lead to specific properties such as better abrasion resistance and lower static and dynamic coefficients of friction (further investigations are already considered) while maintaining acceptable tensile strength of about 45 MPa (Fig. 4a). On the other hand, high rigidity is another key-property required for mechanical applications. It was reported that after the treatments with acids and chemical oxidants [19,20] the graphite sheets contain different functional groups such as ether, hydroxyl, carboxyl, etc. These functional groups are assumed to promote both physical and mechanical/chemical interactions between EG and the polyester matrix. Addition of a nanofiller (graphite) with high modulus (about 1 TPa [21]) leads to a significant reinforcing effect and the increase of rigidity of PLA (initial Young's modulus of 2200 MPa) in direct correlation to EG percentage (Fig. 4b), whereas the nominal strain at break is decreased from 5.8% (neat PLA) to 2.1% (PLA-12% EG).

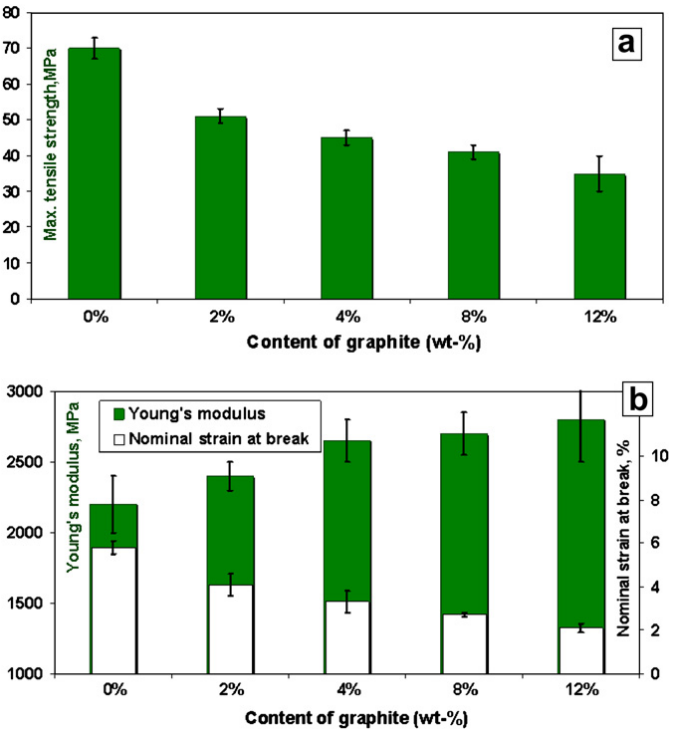

Figure 6. (a, b): Evolution of tensile strength (a), Young's modulus and nominal strain at break (b) for PLA compositions with different contents of EG (direct dosing). (Colour on the Web). [22]

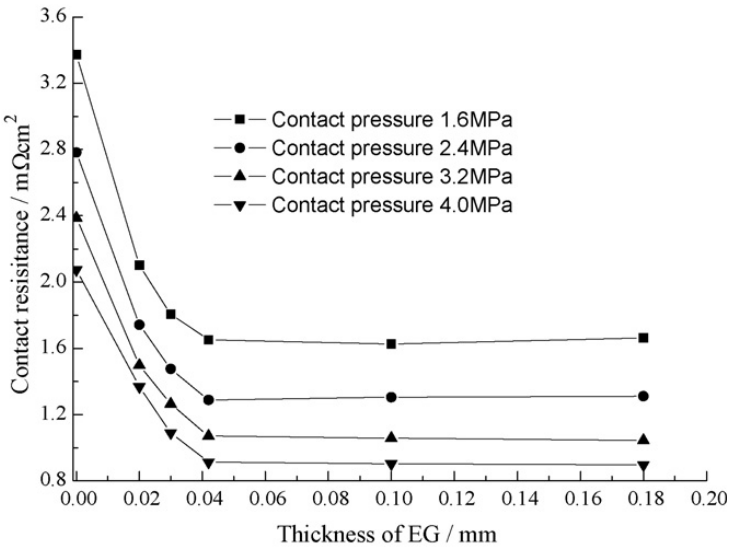

Figure 7: Influence ofEGthickness on contact resistance (PF, 10 wt%; expandedvolume, 150ml g–1) [23].

The effect of contact pressure on the contact resistance of composite plate and GDL was compared under the same thickness conditions as the EG layer (Fig. 7). Higher contact pressure will result in more contacting spots and larger contacting areas. Consequently, the contact resistance decreases as higher contact pressure is exerted [23]. The variation of contact resistance with the thickness of EG at different contact pressures was also studied. The reduction of contact resistance with increasing EG thickness is sharp when the EG layer is thin [23]. As the EG layer become thicker and thicker, the reduction slows down and eventually stops (Fig. 7). Below a certain thickness, it seems that the deformation of the EG layer is not enough to accommodate a full contact with GDL under a given contact pressure. A thicker EG layer permits larger deformation and better contact. But beyond a certain thickness, 40_min our experiments, full contact is realized and further increase in EG thickness makes no improvement. [23]

2.3 PEMFC-bipolar plate

Surface energy of bipolar plates is another important factor to affect cell performance, particularly at high current densities since water produced by the cathode reaction should be properly removed. The bipolar plate with low surface energy is readily flooded at the cathode side of a cell [24]. Contact resistance of three kinds of bipolar plates measured at various compaction pressures. Fig. 8. Static water contact angle of graphite plate, metal composite plate, and expanded graphite plate.energy of the material, water contact angle is measured. The lower the contact angle is, the lower is the surface energy of the material. Fig. 8 exhibits water contact angle of expanded graphite plates is bigger than that of pure graphite plates. Therefore, this expanded graphite bipolar plate can be applied in PEMFC.

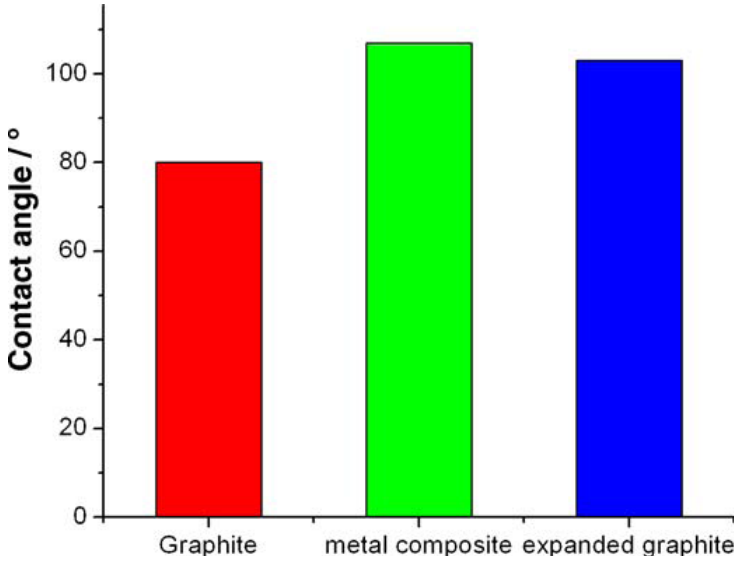

Figure 8: Static water contact angle of graphite plate, metal composite plate, and expanded graphite plate. [25]

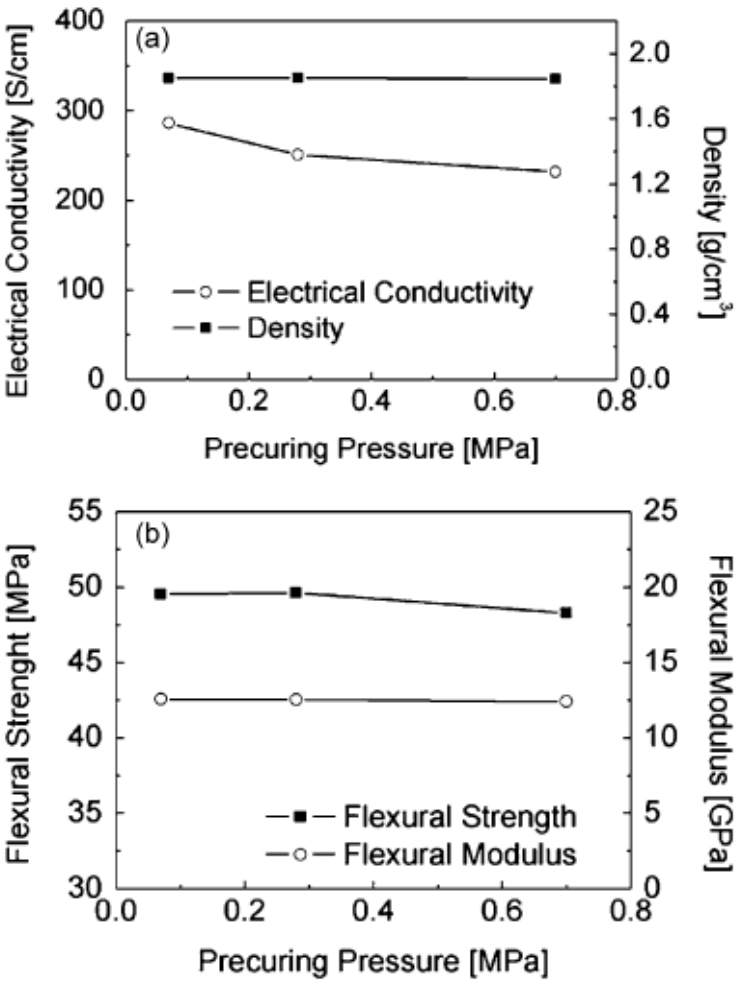

Figure 9: Material properties of composite bipolar plates depending on pre-curing pressure: (a) electrical conductivity and density; (b) flexural strength and modulus. [26]

According to published paper [26], Fig. 9 presents material properties of composite bipolar plates according to the pre-curing pressure. There is no particular change of density regardless of the pre-curing pressure, and the electrical conductivity and flexural strength decrease only slightly as the pre-curing pressure increased. This means that the pre-curing pressure variation, in the 0.07–0.7MPa range, has an insignificant influence on the material properties of composite bipolar plates. Productivity and formability are also important matters. The preform pre-cured below 0.07MPa is likely to break because of a lack of compaction. Therefore, it is difficult to make a preform. As the pre-curing pressure increases from 0.07MPa, the density of the preform increases and finally reaches as high as 1.26 g cm−3 at 0.7MPa. [26]

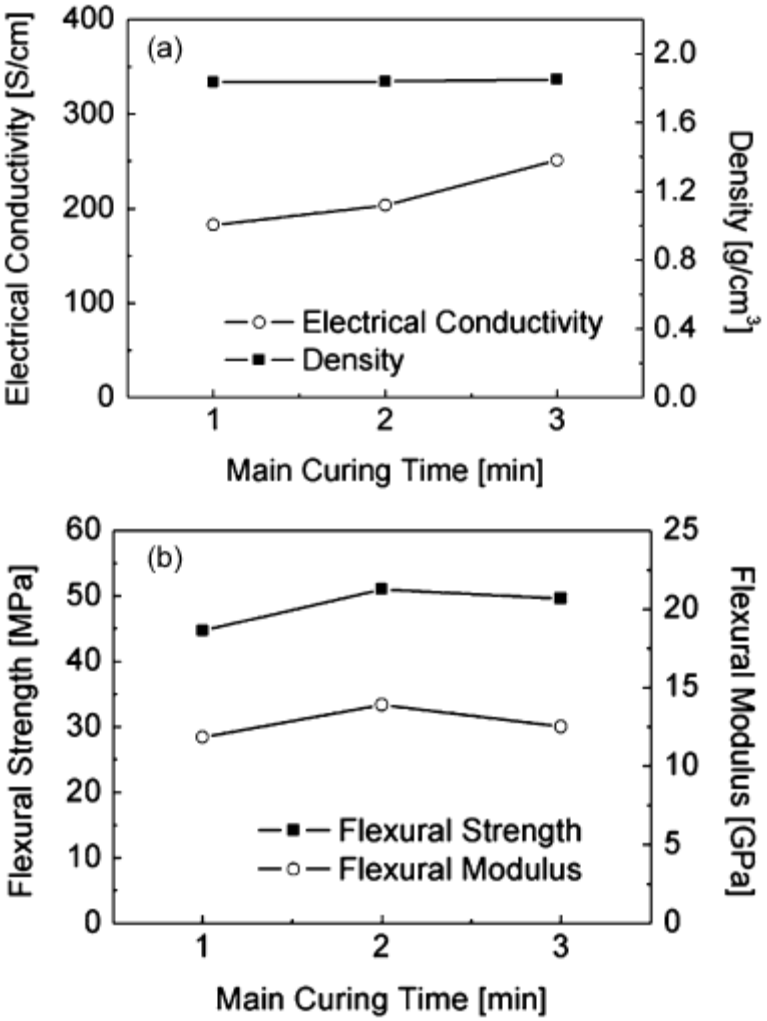

Figure 10: Material properties of composite bipolar plates depending on main curing time: (a) electrical conductivity and density; (b) flexural strength and modulus. [27]

The experimental method was similar to that of the procuring experiment. First, the main curing time was increased from 1 to 3 min at a constant stamping pressure of 10MPa. [27] Fig. 10 presents material properties of composite bipolar plates depending on the main curing time. At 1 min, the flexural strength is low owing to a lack of curing of the phenol resin. While the density is virtually constant, the flexural strength and electrical conductivity reach maxima at 2 and 3 min, respectively. The flexural strength changes very little above the main curing time of 2 min. Hence, a main curing time of 3 min is appropriate for this two-step (preforming and stamping) manufacturing process. Besides merely reducing the high-pressure moulding time compared with existing compression moulding, the perform

moulding technique removes the graphite/phenol dispersion process so that the moulds can always maintain the high temperature [27].

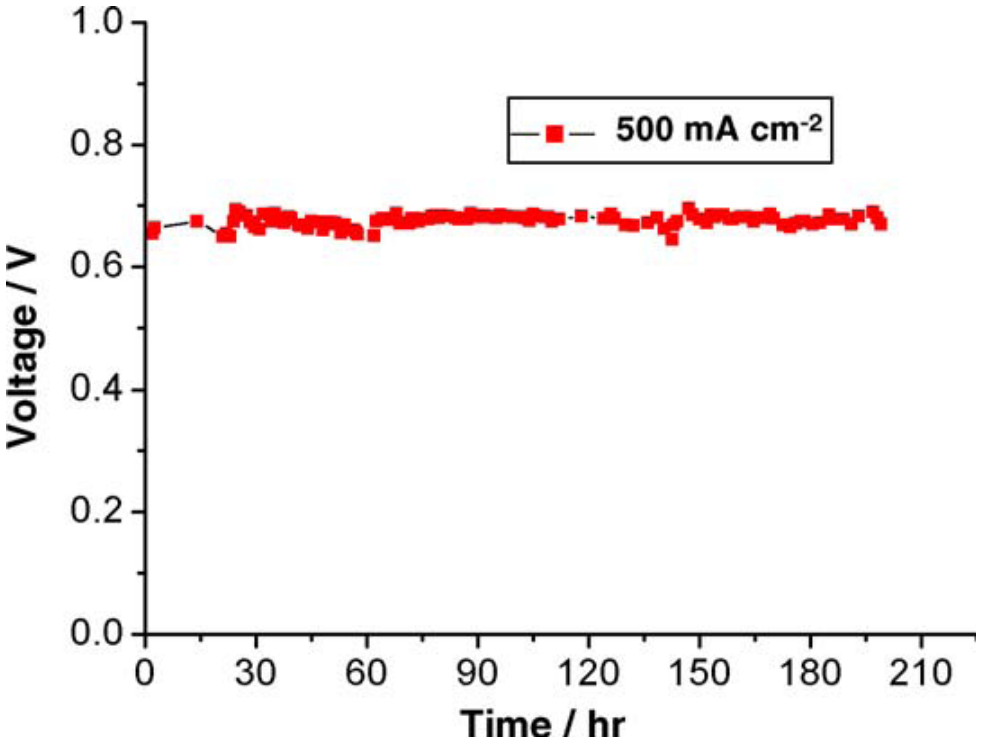

Figure 11: Life-time test of the single fuel cell using the expanded graphite bipolar plate at a constant current density of 500mAcm−2. [28]

Fig. 11 shows the short-term performance of the fuel cell, the fuel cell is operated over 200 h at a constant current density 500mAcm^{-2} [28]. The performance does not degrade obviously, but it is not enough for fuel cell vehicles. The life-time of fuel cell should be over 5000 h if fuel cells are applied in vehicles [28]. Therefore, the durability examination is needed [28].

3. Conclusion

In this investigation, we describe about expanded graphite with expansion ratio of 75–100 cc/gm prepared by chemical oxidation and rapid expansion at high temperature of GIC. Each data reported in the figures are an average value base of experimental results, which shows the repeatability in the propertiesof expanded graphite-based composite application. The composite with varying weight percentage of EG gives the different electrical conductivity, mechanical properties and bulk density. These composite have the critical weight percentage of filler content to achieve desired electrical conductivity and mechanical properties of bipolar plate as per DOE advanced series of target is found to be 50 wt%. The composite

bipolar plate with EG results in bulk density of 1.50 g/cm^3, electrical conductivity 120 S/cm, bending strength 54 MPa, Modulus w6 GPa and shore hardness 50. The lower value of modulus of EG plate as compared with graphite composite plate (>10 GPa) suggest that these plates are more flexible and can better withstand shock and vibration during mobile operation of PEM fuel cell. The flexible bipolar plates can also reduce contact resistance in fuel call stack.

Reference

[1] D.D.L. Chung, Review: graphite, *J. Mater. Sci*. 37 (2002) 1475–1489.

[2] F.Y. Kang, Y.P. Zheng, H.N. Wang, Y. Nishi, M. Inagaki, Effect of preparation conditions on the characteristics of exfoliated graphite, *Carbon* 40 (2002) 1575–1581.

[3] A. Celzard, J.F. Mareche, G. Furdin, Surface area of compressed expanded graphite, *Carbon* 40 (2002) 2713–2718.

[4] Y. Matsuo, Y. Sugie, Preparation, structure and electrochemical properties of pyrolytic carbon from graphite oxide, *Carbon* 36 (1998) 301–303.

[5] A.D. Lucking, L. Pan, D.L. Narayanan, C.E.B. Clifford, Effect of expanded graphite lattice in exfoliated graphite nanofibers on hydrogen storage, *J. Phys. Chem*. B 109 (2005) 12,710–12,717.

[6] A. Bhattacharya, A. Hazra, S. Chatterjee, P. Sen, S. Laha, I. Basumallick, Expanded graphite as an electrodematerial for an alcohol fuel cell, *J. Power Sources* 136 (2004) 208–210.

[7] C. Calas-Blanchard, T. Noguer, M. Comtat, S. Mauran, J.L. Marty, Potentialities of expanded natural graphite as a newtransducer forNAD+-dependent dehydrogenase amperometric biosensors, *Anal. Chim. Acta* 484 (2003) 25–31.

[8] W. Li, C. Han, W. Liu, M.H. Zhang, K.Y. Tao, Expanded graphite applied in the catalytic process as a catalyst support, *Catal. Today* 125 (2007) 278–281.

[9] W.C. Shen, S.Z.Wen,N.Z. Cao, L. Zheng,W. Zhou, Y.J. Liu, J.L. Gu, Expanded graphite—a new kind of biomedical material, *Carbon* 37 (1999) 356–358.

[10] B. Tryba, J. Przepiorski, A.W. Morawski, Influence of chemically prepared H2SO4–graphite intercalation compound (GIC) precursor on parameters of exfoliated graphite (EG) for oil sorption from water, *Carbon* 41 (2003) 2012–2015.

[11] S.R. Dhakate, S. Sharma, M. Borah, R.B. Mathur, T.L. Dhami, Expanded graphite-based electrically conductive composites as bipolar plate for PEM fuel cell, *International Journal of Hydrogen Energy*, 33 (2008) 7146 – 7152.

[12] Mingfei Zhao, Peng Liu, Adsorption of methylene blue from aqueous solutions by modified expanded graphite powder, *Desalination* 249 (2009) 331–336.

[13] Xueqing Yue, Liang Li, Ruijun Zhang, Fucheng Zhang, Effect of expansion temperature of expandable graphite on microstructure evolution of expanded graphite during high-energy ball-milling, *Materials Characterization*, 60 (2009) 1541–1544.

[14] Chen Y, Gerald JF, Chadderton LT, Chaffron L. Nanoporous carbon produced by ball-milling. *Appl Phys Lett*. 1999; 74:2782–4.

[15] Huang JY. HRTEM and EELS studies of defects structure and amorphous-like graphite induced by ball-milling. *Acta Mater 1999*; 47:1801–8.

[16] Inagaki M, Tashiro R, Washino Y, Toyoda M. Exfoliation process of graphite via intercalation compounds with sulfuric acid. *J Phys Chem Solids* 2004; 65:133–7.

[17] Francke M, Hermann H, Wenzel R, Seifert G, Wetzig K. Modification of carbon nanostructures by high energy ball-milling under argon and hydrogen atmosphere. *Carbon* 2005; 43:1204–12.

[18] Reynolds III RA, Greinke RA. Influence of expansion volume of intercalated graphite on tensile properties of flexible graphite. *Carbon* 2001; 39:473–81.

[19] Hussain F, Hojjati M, Okamoto M, Gorga RE. Polymer-matrix nanocomposites, processing, manufacturing, and application: an overview. *J Compos Mater* 2006; 40(17):1511e75.

[20] Yasmin A, Luo JJ, Daniel IM. Processing of expanded graphite reinforced polymer nanocomposites. *Compost Sci Technol* 2006; 66(9):1182e9.

[21] Chen G, Weng W, Wu D, Wu C. PMMA/graphite nanosheets composite and its conducting properties. *Eur Polym J* 2003; 39(12):2329-35.

[22] Marius Murariu, Anne Laure Dechief, Leila Bonnaud, Yoann Paint, Antoine Gallos, Gaëlle Fontaine, Serge Bourbigot, Philippe Dubois, The production and properties of polylactide composites filled with expanded graphite, *Polymer Degradation and Stability* 124 (2010) 1-12.

[23] Dongjie Li, YuxinWang, Li Xu, Jun Lu, QianWu, Surface modification of a natural graphite/phenol formaldehyde composite plate with expanded graphite, *Journal of Power Sources* 183 (2008) 571–575.

[24] A.J. Cisar, O.J. Murphy, K.-I. Jeng, S. Simpson, D. Weng, *US Patent* 6, 426,161 (2002).

[25] Xiqiang Yan, Ming Hou, Haifeng Zhang, Fenning Jing, Pingwen Ming, Baolian Yi, Performance of PEMFC stack using expanded graphite bipolar plates, *Journal of Power Sources* 160 (2006) 252–257.

[26] S.I. Heo, K.S. Oh, J.C. Yun, S.H. Jung, Y.C. Yang, K.S. Han, Development of preform moulding technique using expanded graphite for proton exchange membrane fuel cell bipolar plates, *Journal of Power Sources* 171 (2007) 396–403.

[28] Xiqiang Yan, Ming Hou, Haifeng Zhang, Fenning Jing, Pingwen Ming, Baolian Yi, Performance of PEMFC stack using expanded graphite bipolar plates, *Journal of Power Sources* 160 (2006) 252–257.